Regioselectivity of the Nucleophilic Addition to (η^3-allyl) Palladium Complexes. A Theoretical Study

F. Delbecq* and C. Lapouge

Institut de Recherches sur la Catalyse, 2 Avenue A. Einstein, 69626 Villeurbanne Cédex, France, and Ecole Normale Supérieure de Lyon, 46 Allée d'Italie, 69364 Lyon Cédex 07, France

Received April 10, 2000

Density functional calculations were performed to study the factors influencing the regioselectivity of the nucleophilic attack at allyl−Pd complexes disymmetrically substituted by electron-donating groups. The geometries of the reactants and of the products obtained after NH_3 addition were fully optimized, and the transition states were localized. The more disymmetrical the allylic complex, the more regioselective the reaction toward the substituted carbon. An explanation is given based on the shapes of the LUMO and HOMO of the allylic complexes. Results in better agreement with the experiments are obtained if solvent effects are introduced.

1. Introduction

The palladium-catalyzed allylic alkylation reaction has been extensively used in the past decades for the formation of carbon−carbon or carbon−heteroatom bonds. The key intermediate in this reaction is a (η^3-allyl)Pd(II) complex, easily attacked by nucleophiles at its allylic moiety. This reaction is more and more used now in enantioselective synthesis by means of chiral ligands on palladium.

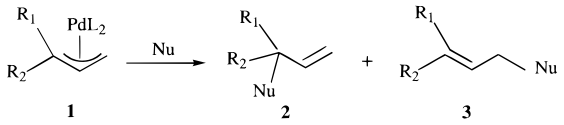

1 **2** **3** (1)

Numerous experimental studies exist on the subject (see for example ref 2 in ref 1). The problem of regioselectivity is crucial, that is, the orientation of the nucleophilic attack that gives **2** or **3** (eq 1). From the various experimental data it is difficult to extract rules if only electron-donating substituents are considered. For example the isomeric cis−trans geranyl and neryl allylic complexes give opposite regioselectivities.[2] The steric effects seem to play an important role. Nevertheless, for not too bulky substituents, some trends exist: when the allyl part is monosubstituted by a methyl (R_1 = H, R_2 = CH_3), the nucleophile binds mainly at the nonsubstituted carbon, and when it is dimethylated (R_1 = R_2 = CH_3), the nucleophile binds rather at the substituted carbon.[3,4] On the contrary, for an allylic complex monosubstituted by a methoxy group (R_1 = H, R_2 = OCH_3), the regioselectivity is totally inverted and the only product is **2**.[5] Therefore, apart from the steric effects, the electronic effects must play a role in the direction of the nucleophilic attack. The study of these effects is the purpose of the present work.

To our knowledge, the previous theoretical works on the (η^3-allyl) palladium complexes deal with the ligands effects rather than with the allylic substituent effects. Most of these calculations have been carried out on a semiempirical level.[6−8] For our part, we have already addressed the problem of substituent effects by means of extended Hückel type calculations.[9] The conclusion of these semiempirical studies is that the reaction is controlled by the frontier orbitals rather than by the charges. For the past few years, ab initio calculations have been performed on the (η^3-allyl) palladium complexes (among them 10−14; for an exhaustive review see ref 15). Very recently, the electronic effects of substituents on the allyl have been investigated in the case of 1,3-diaryl (η^3-allyl) palladium complexes.[16]

The purpose of the present work was to carry out ab initio calculations on (η^3-allyl) palladium complexes substituted on one carbon by electron-donating groups in order to understand the opposite regioselectivities observed experimentally. Besides the unsubstituted case **1d** (R_1 = R_2 = H), three complexes have been considered: **1a** with R_1 = H and R_2 = CH_3, **1b** with R_1 = H and R_2 = OCH_3, and **1c** with R_1 = R_2 = CH_3 (see Scheme 1). To save computational time, the ligands on Pd were modeled by PH_3. The most common experimental nucleophiles are stabilized carbanions, but neutral nucleo-

* Corresponding author. E-mail: delbecq@catalyse.univ-lyon1.fr. Tel: (33) 4 72 44 53 52.

(1) Trost, B. M.; Bunt, R. C. *J. Am. Chem. Soc.* **1998**, *120*, 70.
(2) Trost, B. M.; Verhoeven, T. R. *J. Am. Chem. Soc.* **1980**, *102*, 4730.
(3) Åkermark, B.; Åkermark, G.; Hegedus, L.-S.; Zetterberg, K. *J. Am. Chem. Soc.* **1981**, *103*, 3037.
(4) Åkermark, B.; Hansson, S.; Krakenberger, B.; Vitagliano, A.; Zetterberg, K. *Organometallics* **1984**, *3*, 679.
(5) (a) Vicart, N.; Cazes, B.; Gore, J. *Tetrahedron Lett.* **1995**, *36*, 535. (b) Yamamoto, Y.; Al-Masum, M. *Synlett* **1995**, 969.
(6) Shilling, B. E. R.; Hoffmann, R.; Faller, J. N. *J. Am. Chem. Soc.* **1979**, *101*, 592.
(7) Curtis, M. D.; Eisenstein, O. *Organometallics* **1984**, *3*, 887.
(8) Ward, T. R. *Organometallics* **1996**, *15*, 2836.
(9) Bigot, B.; Delbecq, F. *New J. Chem.* **1990**, *14*, 659.
(10) Blöchl, P. E.; Togni, A. *Organometallics* **1996**, *15*, 4125.
(11) Szabo, K. J. *J. Am. Chem. Soc.* **1996**, *118*, 7818.
(12) Hagelin, H.; Åkermark, B.; Norrby, P.-O. *Chem. Eur. J.* **1999**, *5*, 902.
(13) Szabo, K. J. *Organometallics* **1996**, *15*, 1128.
(14) Aranyos, A.; Szabo, K. J.; Castano, A. M.; Bäckvall, J. E. *Organometallics* **1997**, *16*, 1058.
(15) Dedieu, A. *Chem. Rev.* **2000**, *100*, 543.
(16) Branchadell, V.; Moreno-Manas, M.; Pajuelo, F.; Pleixats, R. *Organometallics* **1999**, *18*, 4934.

10.1021/om0003032 CCC: $19.00
Publication on Web 06/03/2000

Scheme 1. The Four Studied Reactions

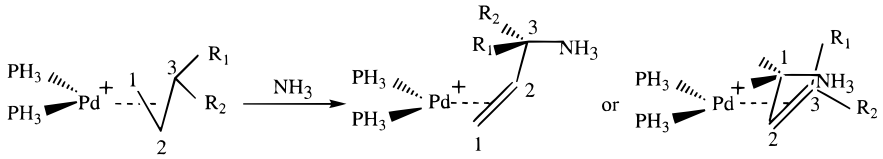

1 **2** **3**

1a $R_1 = H, R_2 = CH_3$ **1c** $R_1 = R_2 = CH_3$
1b $R_1 = H, R_2 = OCH_3$ **1d** $R_1 = R_2 = H$

philes such as amines are often used. We chose NH_3 as a nucleophile since the use of an anion like CH_3^- requires a large basis set with diffuse functions. Moreover, it is generally admitted that the starting (η^3-allyl)-Pd(II) complex is cationic and the reaction between ionic species is not well described in the gas phase. Hence the reaction studied in the present work is described in Scheme 1. After fixation of NH_3 on the allylic part, a cationic olefin complex is obtained with a quaternary ammonium. The latter complex leads to the amino-substituted olefin after decoordination and loss of a proton.

For the first time, the geometries of the reactants and products were determined. Then the transition states were located and compared. Finally a qualitative interpretation is given.

2. Computational Methods

The calculations were based on the density functional theory (DFT) at the generalized gradient appromixation (GGA). They were performed with the Gaussian 94 and Gaussian 98 programs.[17−18] The chosen functional was the hybride one B3LYP,[19] which was shown to give results comparable to those of MP2 calculations.[20] For Pd and P, the relativistic effective core potentials of Hay and Wadt were used with the corresponding double-ζ basis set.[21] For P a d function was added ($\alpha = 0.37$). For C, N, O, and H the Dunning−Huzinaga valence double-ζ basis set was used[22] with an added d function on C, N, and O (D95V*). The geometries were fully optimized using the gradient technique. The transition states (TS) were searched with the QST3 algorithm. All the minima and TS were then characterized by frequency calculations which gave the number of imaginary frequencies and allowed us to have the zero-point energies (ZPE). Finally intrinsic reaction coordinate (IRC) calculations showed that the TS found connect effectively the reactants and products.

In the studied reaction involving a cationic complex, the solvation must play an important role. It has been shown recently[12] that the reaction between an anionic nucleophile and a cationic allyl−palladium complex does not have any transition state in the gas phase. The consideration of solvent effects allows the authors to obtain a barrier. In one of our cases ($R_2 = OCH_3$) we also found no barrier in the gas phase (vide infra). Therefore we introduced solvent effects in our calculations. We chose the polarizable continuum model of Tomasi, which considers the solute in a cavity of solvent only represented by its dielectric constant.[23]

For weakly bound species, as are the two molecules in a transition state, the basis set superposition error (BSSE) can be important. For the last few years, mechanistic calculations of organometallic reactions have taken the BSSE into account,[24−26] although the introduction of the BSSE can be controversial.[27] For calculating the BSSE we used the counterpoise method of Boys and Bernadi,[28] which is known to overestimate the BSSE.[26] We estimated the BSSE as the difference between the energies of the two molecules calculated in the TS geometry with the whole basis set and their energies calculated in the same geometry but with their own basis set.

3. Results

a. Geometries of the (η^3-allyl) Palladium Complexes 1a−d. Besides the three complexes given in Scheme 1, we also optimized the geometry of the (η^3-allyl)$Pd(PH_3)_2^+$ complex **1d**, which has no substituents on the allyl. The four complexes are represented in Figure 1 with the main geometrical parameters obtained after optimization. Our values differ slightly from those found at the MP_2 level for **1a**[11] and **1d**[29] but are in rather good agreement with the experimental data. In the case of **1d** for instance, we found a dihedral angle of 111.52° between the allyl plane and the PdC_1C_3 plane; C_1 and C_3 are 0.15 Å above the PPdP plane and C_2 is 0.48 Å below this plane. Experimentally, the allyl plane is inclined at 111.5° to the PdClPd plane in [(η_3-allyl)-$PdCl]_2$,[30] the central carbon is 0.58 Å below this plane, and the terminal carbons are between 0.1 and 0.05 Å above it. In **1a** C_1 and C_3 are 0.13 and 0.20 Å above the PPdP plane, respectively, and C_2 is 0.47 Å below it. In

(17) Frisch, M. J.; Trucks, G. W.; Schlegel, H. B.; Gill, P. M. W.; Johnson, B. G.; Robb, M. A.; Cheeseman, J. R.; Keith, T.; Petersson, G. A.; Montgomery, J. A.; Raghavachari, K.; Al-Laham, M. A.; Zakrzewski, V. G.; Ortiz, J. V.; Foresman, J. B.; Cioslowski, J.; Stefanov, B. B.; Nanayakkara, A.; Challacombe, M.; Peng, C. Y.; Ayala, P. Y.; Chen, W.; Wong, M. W.; Andres, J. L.; Replogle, E. S.; Gomperts, R.; Martin, R. L.; Fox, D. J.; Binkley, J. S.; Defrees, D. J.; Baker, J.; Stewart, J. P.; Head-Gordon, M.; Gonzalez, C.; Pople, J. A. *Gaussian 94*, revision B.1; Gaussian, Inc.: Pittsburgh, PA, 1995.

(18) Frisch, M. J.; Trucks, G. W.; Schlegel, H. B.; Scuseria, G. E.; Robb, M. A.; Cheeseman, J. R.; Zakrzewski, V. G.; Montgomery, J. A., Jr.; Stratmann, R. E.; Burant, J. C.; Dapprich, S.; Millam, J. M.; Daniels, A. D.; Kudin, K. N.; Strain, M. C.; Farkas, O.; Tomasi, J.; Barone, V.; Cossi, M.; Cammi, R.; Mennucci, B.; Pomelli, C.; Adamo, C.; Clifford, S.; Ochterski, J.; Petersson, G. A.; Ayala, P. Y.; Cui, Q.; Morokuma, K.; Malick, D. K.; Rabuck, A. D.; Raghavachari, K.; Foresman, J. B.; Cioslowski, J.; Ortiz, J. V.; Stefanov, B. B.; Liu, G.; Liashenko, A.; Piskorz, P.; Komaromi, I.; Gomperts, R.; Martin, R. L.; Fox, D. J.; Keith, T.; Al-Laham, M. A.; Peng, C. Y.; Nanayakkara, A.; Gonzalez, C.; Challacombe, M.; Gill, P. M. W.; Johnson, B. G.; Chen, W.; Wong, M. W.; Andres, J. L.; Head-Gordon, M.; Replogle, E. S.; Pople, J. A. *Gaussian 98*, revision A.5; Gaussian, Inc.: Pittsburgh, PA, 1998.

(19) Becke, A. D. *J. Chem. Phys.* **1993**, *98*, 5648.

(20) (a) Foresman, J. B.; Frisch, A. E. *Exploring Chemistry with Electronic Structure Methods*, 2nd ed.; Gaussian Inc.: Pittsburgh, 1996. (b) Singleton, D. A.; Merrigan, S. R.; Liu, J.; Houk, K. N. *J. Am. Chem. Soc.* **1997**, *119*, 3385.

(21) Hay, P. J.; Wadt, W. R. *J. Chem. Phys.* **1985**, *85*, 299.

(22) Dunning, T. H., Jr.; Hay, P. J. In *Modern Theoretical Chemistry*; Schaefer, H. F., III, Ed., Plenum: New York, 1976; pp 1−28.

(23) Tomasi, J.; Persico, M. *Chem. Rev.* **1994**, *94*, 2027.

(24) Frankcombe, K. E.; Cavell, K. J.; Yates, B. F.; Knott, R. B. *J. Phys. Chem.* **1996**, *100*, 18363.

(25) Musashi, Y.; Sakaki, S. *J. Chem. Soc., Dalton Trans.* **1998**, 577.

(26) Sakaki, S.; Biswas, B.; Sugimoto, M. *Organometallics* **1998**, *17*, 1278.

(27) Lendvay, G.; Mayer, I. *Chem. Phys. Lett.* **1998**, *297*, 365.

(28) Boys, S. F.; Bernardi, F. *Mol. Phys.* **1970**, *19*, 553.

(29) Sakaki, S.; Takeuchi, K.; Sugimoto, M.; Kurosawa, H. *Organometallics* **1997**, *16*, 2995.

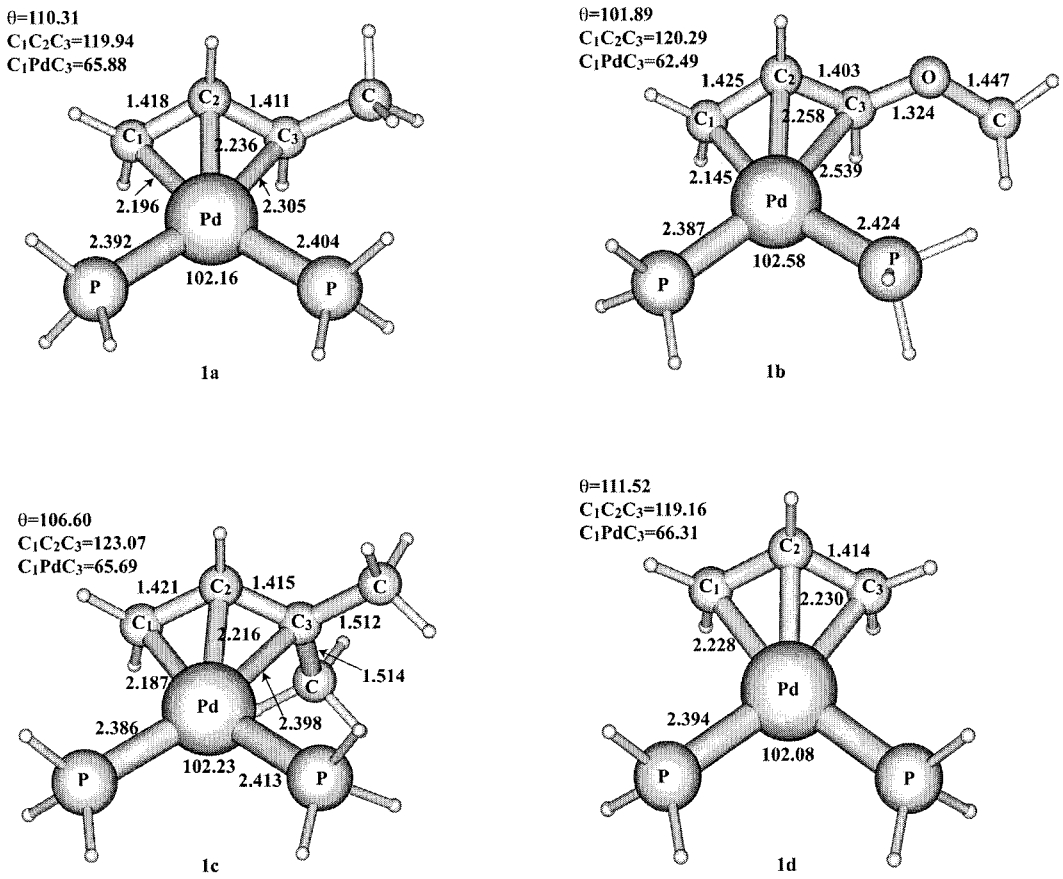

Figure 1. Main geometrical optimized parameters of the (η_3-allyl)Pd complexes **1a**−**d**.

1b and **1c**, C_1 is in the PPdP plane, C_2 is 0.48 Å below it, and C_3 is 0.40 and 0.28 Å above it, respectively. Thus when the substituents change, the central carbon keeps a fixed position below the complex plane and C_1C_3 pivots all the more that the PdC_3 bond is weaker. The substituents on C_1 and C_3 are significantly bent away from the metal. The anti hydrogen on the nonsubstituted carbon is bent by 33.3°, 28.7°, 32.1°, and 33.4° in **1a**−**d**, respectively and on the substituted carbon by 27.4°, 15.7°, 30.3° ($R_1 = CH_3$), and 33.3° respectively. The syn hydrogen (on the nonsubstituted carbon) is bent by 8°, −2°, 6°, and 10°, respectively, and R_3 by 27.4°, 15.7°, 30.3°, and 33.3° respectively. Such bendings are consistent with previous experimental data.[31]

The most interesting fact to be noted is that the substituted carbon is farther from the palladium atom than the nonsubstituted one. The difference between the PdC_1 and PdC_3 bond lengths increases in the order **1a** (0.11 Å), **1c** (0.21 Å), and **1b** (0.39 Å). At the same time, the C_1C_2 bond length becomes longer than the C_2C_3 one, indicating a weaker double-bond character for C_1C_2. Therefore, when the allyl moiety is disymmetrically substituted, the structure of the (η_3-allyl)$Pd(PH_3)_2^+$ complex is distorted, with a stronger bond between the metal and the nonsubstituted carbon. This has been found experimentally in the case of a phenyl substituent.[31]

b. Geometries of the Olefin−Palladium Complexes 2a−d and 3a−c. The seven olefin complexes

Scheme 2. Shape of the Olefin π*CC Orbital in Interaction with the Pd d Orbital in Complexes 2 or 3

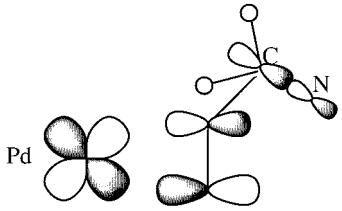

obtained after fixation of NH_3 on the allyl terminal carbons are described in Figure 2 (for **1d** only one exits) with the main optimized geometrical parameters. When the olefin is monosubstituted (cases of complexes **2**), the substituted carbon is always farther from Pd. In all cases the ethylenic bond C_1C_2 or C_2C_3 is elongated with similar values (1.424−1.430 Å). These values as well as the PdC bonds are in agreement with the X-ray experimental data.[32] The ethylenic carbons are slightly below the PPdP plane by 0.01−0.15 Å. Hence the complexes are quasi square planar (maximum deviation 4°). The ethylenic carbons are hybridized toward sp^3: the substituents are all bent away from the metal by 10−13°.

In all cases except **2b**, the CN bond length is 1.59−1.60 Å. A rotation around C_2C_3 in **2** or C_1C_2 in **3** shows that other minima exist with NH_3 pointing toward Pd ($\theta = -137°$ for **3** and 126° for **2**). In these second minima the CN bond is smaller (ca. 1.54 Å) but remains larger

(30) Smith, A. E. *Acta Crystallogr.* **1965**, *18*, 331.
(31) Murrall, N. W.; Welch, A. J. *J. Organomet. Chem.* **1986**, *301*, 109.
(32) Werner, H.; Crisp, G. T.; Jolly, P. W.; Kraus, H. J.; Krüger, C. *Organometallics* **1983**, *2*, 1369.

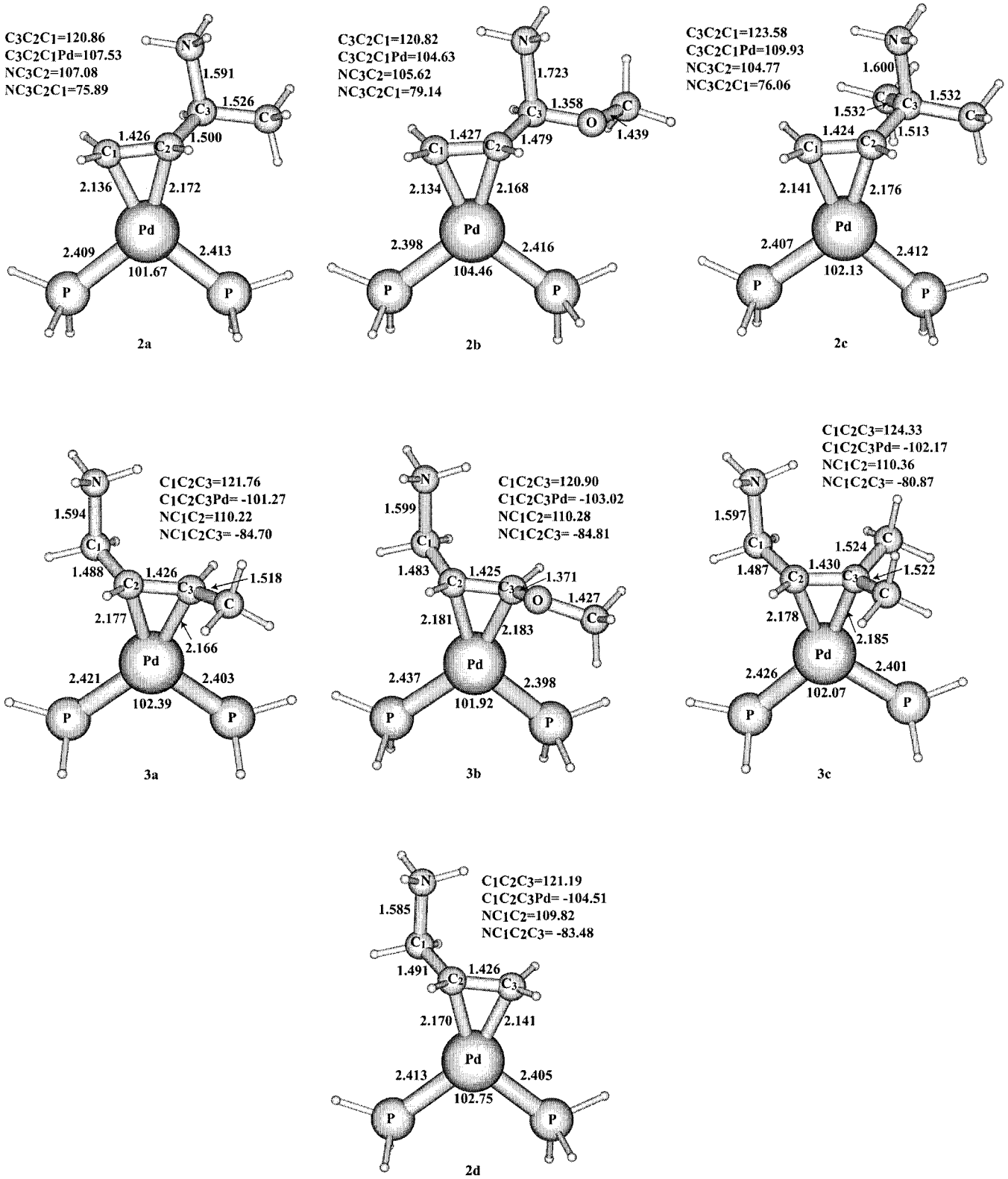

Figure 2. Main geometrical optimized parameters of the olefin−Pd complexes **2a**−**d** and **3a**−**c**.

than the usual CN length because of the character of quaternary ammonium. Why is the CN bond larger when NH_3 is opposite Pd? The π*CC orbital mixes with the σ*CN orbital, which is relatively low in energy.

In ethylenic complexes one of the main orbital interactions is between the d_{xy} orbital of the metal and the π*CC orbital (Scheme 2). This interaction results in an electronic transfer into the π*CC orbital (back-donation) and hence in a filling of σ*CN, which leads to the CN lengthening. The same effect is observed for the CH bond trans to the metal in the second minima. However in this case the lengthening is small (0.002 Å) because the σ*CH orbital is high and mixes only weakly with π*CC. When NH_3 is adjacent to OCH_3 (**2b**), the CN bond is even more elongated (1.723 Å) because of a repulsive interaction between N and an oxygen lone pair (there is a negative overlap population between O and N).

c. Geometries of the Transition States TS2a−d

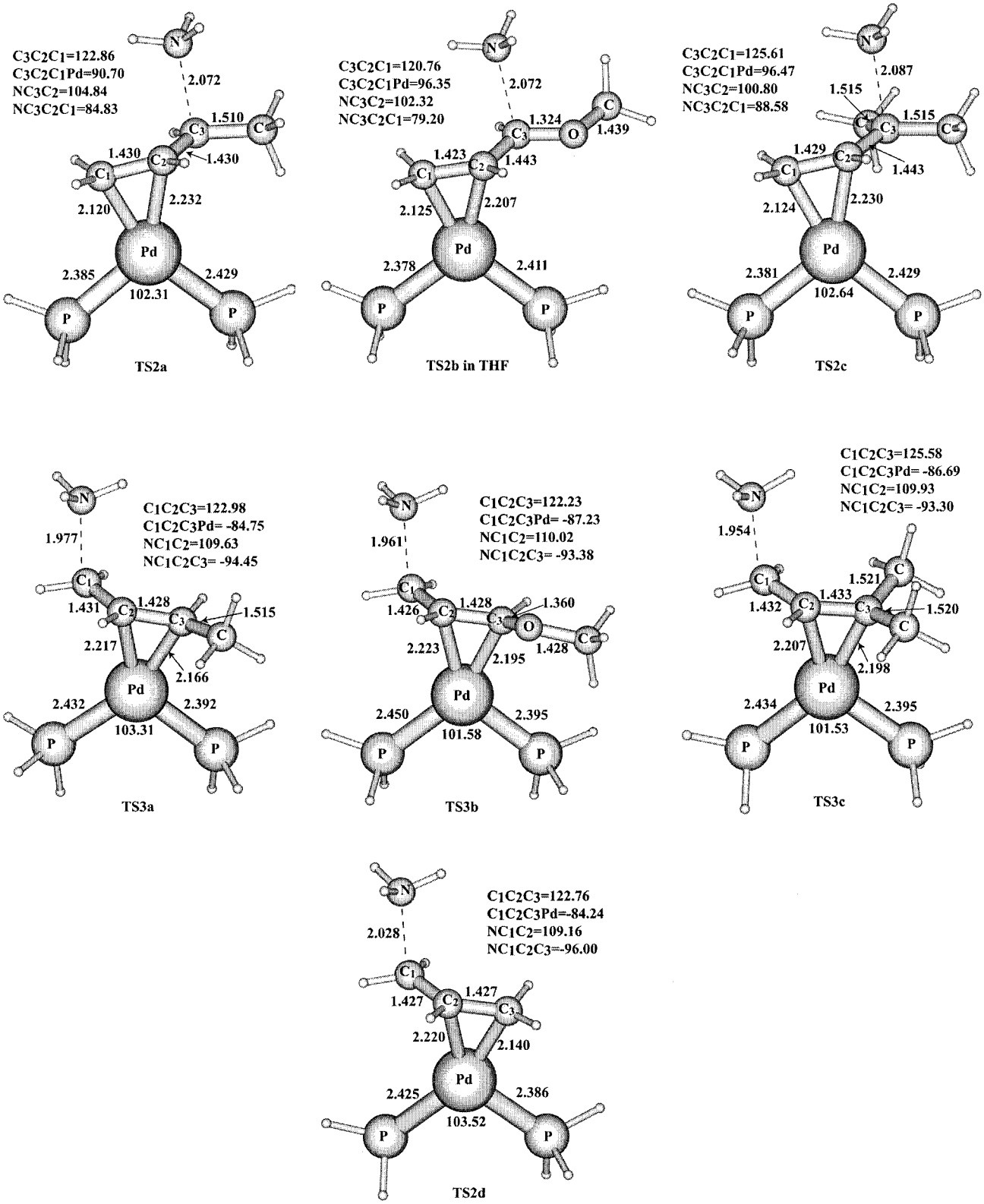

Figure 3. Main geometrical optimized parameters of the transition states **TS2a**−**d** and **TS3a**−**c**. For **TS2b**, the given geometry is that obtained in THF since no TS was obtained in the gas phase (see text).

and TS3a−**c.** The transition states connecting **1a**−**d** to **2a**−**d** are called **TS2a**−**d**, and those connecting **1a**−**c** to **3a**−**c** are called **TS3a**−**c** (there is only one TS for **1d**). They are drawn in Figure 3 with the main optimized parameters. In the case of **1b** ($R_2 = OCH_3$), no transition state (**TS2b**) could be found for attack on the substituted carbon (the geometry shown in Figure 3 was obtained in THF (vide infra)). A scan performed by varying the C−N bond length and optimizing all the other parameters gives a curve connecting **1b** and **2b** with a nonsignificant barrier. One can observe that N is farther from C in **TS2** (attack on the substituted C) than in **TS3** (attack on the nonsubstituted C). The comparison of Figures 2 and 3 allows us to conclude that

Table 1. Reaction Energies ΔE (E_2 or $E_3 - E_1$) and Barrier Energies E^*(E_{TS2} or $E_{TS3} - E_1$) and ΔE^*($E_{TS2} - E_{TS3}$) in kcal/mol[a]

	ΔE_2	E^*_2	ΔE_3	E^*_3	ΔE^*(3−2)
a	1.9	4.2 (6.2)	4.2	5.3 (7.3)	1.0 (1.2)
b	3.7	0	7.9	8.5 (10.5)	8.5 (10.5)
c	2.4	4.5 (6.8)	6.3	7.1 (9.2)	2.5 (2.4)
d[b]	0.5	2.6 (4.4)			

[a] The energies are corrected by ZPE. For the TS, the ΔE^* values corrected by BSSE are given in parentheses. [b] For the nonsubstituted allyl moiety only one reaction exists.

the transtion states are "late", which means that they have geometries near those of the final olefin complexes. Similar TS structures have been obtained previously for complexes bearing different ligands and different allyl moieties.[10,12]

d. Energetics of the Reaction. In Table 1 are collected the reaction energies ΔE (difference between the energies of **2** or **3** and **1**) and the reaction barriers E^* (difference between the energies of **TS2** or **TS3** and **1**). All the energies are corrected by the zero-point energies (ZPE). The energies of the TS are further corrected by the BSSE (see Computational Methods). These results correspond to a gas-phase reaction. One observes only that the reactions are endothermic ($\Delta E > 0$), as it has also been found previously for attack of NH_3 on a P, N complex[10] and on **1d**.[12] In the latter case we found the same ΔE value (2 kJ/mol).

Except for the attack at the substituted carbon of **1b**, which proceeds without barrier, all the activation energies E^* are larger for the substituted allyls than for allyl itself. The BSSE correction varies only a little from one TS to the other (from 1.84 to 2.22 kcal/mol). Therefore it has no influence on the relative energies. In the three (a, b, c) cases, the barrier E^* is greater for **TS3** than for **TS2**, which means that the nucleophile attack is always preferred at the substituted carbon.

The regioselectivity decreases with ΔE^* (see Table 1), and the NH_3 attack at **1b** ($R_2 = OCH_3$) is more regioselective than at **1c** ($R_1 = R_2 = CH_3$) and much more than at **1a** ($R_2 = CH_3$). This order respects the trends of the experimental data. Nevertheless the ΔE^* values are too large and give a too large preference to the substituted carbon.

e. Solvent Effects. As we said in section 2, the solvent effects can have a great influence in determining the transition states of reactions involving ionic species. We therefore introduced solvent effects in our calculations by means of the PCM model of Tomasi et al. (polarizable continuum model). We chose THF and DMSO as solvents because they are the most used experimentally. Their dieletric constants are 7.58 and 46.7, respectively.

We reoptimized all reactants, products, and transition states and performed frequency calculations. This allows us to do the ZPE correction. We have also calculated the BSSE correction for the new geometries of the transition states. Then we obtained energies comparable to those of Table 1. For the reactants, the (η_3-allyl)Pd complexes, the geometry does not change much when the solvent effects are taken into account. There is a general small shortening of the bonds (less than 0.01 Å). The PdC_3 bond is a little more affected: 0.02 Å for **1a**, 0.03 Å for **1b**, and 0.04 Å for **1c**. For the products, the olefin−Pd complexes, the geometry does not change much either. All bonds are a little lengthened except the double bond (C_1C_2 in **2** and C_2C_3 in **3**), which is shortened by around 0.01 Å. That means that its interaction with Pd is slightly weakened. The effects are a little larger for DMSO. The C−N bond length is much affected because of the solvent effect on the quaternary ammonium: it is shortened by 0.03−0.04 Å for all complexes and even more for **2b** (0.12 Å). Effectively for the latter case, the CN bond, which was unexpectively long (1.723 Å), is shortened to 1.601 Å in THF and 1.591 Å in DMSO, values close to those obtained in the other complexes. This can be explained by the solvation of the oxygen pairs, which have a less repulsive interaction with the nitrogen.

Table 2. Main Optimized Geometrical Parameters of the Transition States TS2a−c and TS3a−c in THF and DMSO (bonds in Å, angles in deg)

		TS2a	TS2b	TS2c	TS3a	TS3b	TS3c
PdC_1	THF	2.133	2.125	2.132	2.620	2.643	2.649
	DMSO	2.135	2.125	2.135	2.602	2.618	2.624
PdC_2	THF	2.233	2.207	2.225	2.223	2.236	2.212
	DMSO	2.231	2.212	2.223	2.222	2.238	2.212
PdC_3	THF	2.756	2.957	2.878	2.185	2.227	2.217
	DMSO	2.736	2.940	2.861	2.189	2.234	2.223
C_1C_2	THF	1.425	1.423	1.426	1.419	1.415	1.420
	DMSO	1.423	1.422	1.425	1.419	1.415	1.418
C_2C_3	THF	1.420	1.443	1.428	1.421	1.420	1.427
	DMSO	1.417	1.439	1.426	1.420	1.419	1.426
CN	THF	2.218	2.072	2.258	2.134	2.115	2.113
	DMSO	2.254	2.122	2.282	2.151	2.135	2.139
NCC	THF	103.35	102.34	98.29	108.51	108.98	108.89
	DMSO	102.57	101.93	97.79	108.16	108.67	108.55
θ[a]	THF	88.24	79.00	94.39	−100.11	−97.82	−99.14
	DMSO	89.07	79.17	95.04	−100.71	−98.24	−99.95

[a] θ = dihedral angle $NC_3C_2C_1$ or $NC_1C_2C_3$.

Table 3. Reaction Energies ΔE (E_2 or $E_3 - E_1$) and Barrier Energies E^*(E_{TS2} or $E_{TS3} - E_1$) and ΔE^*($E_{TS2} - E_{TS3}$) in THF and DMSO (in kcal/mol)[a]

		ΔE_2	E^*_2	ΔE_3	E^*_3	ΔE^*(3−2)
a	THF	−2.0	7.6 (9.3)	−1.2	6.1 (7.8)	−1.5 (−1.5)
	DMSO	−2.6	6.4 (8.1)	−2.8	6.1 (7.9)	−0.2 (−0.2)
b	THF	0.7	3.2 (5.7)	1.7	8.4 (10.0)	5.2 (4.3)
	DMSO	−0.6	3.2 (5.3)	0.3	8.3 (10.1)	5.2 (4.7)
c	THF	−0.7	6.4 (8.3)	0.6	7.3 (9.1)	0.9 (0.8)
	DMSO	−1.2	6.9 (8.8)	−0.4	7.5 (9.3)	0.6 (0.5)

[a] All values are corrected by ZPE. The BSSE corrected energies are given in parentheses.

The geometries of the transition states change more. They are given in Table 2. The first remark is that a TS could be located for the attack at the substituted carbon of **1b**, whereas no TS was obtained without solvent. Second the C−N bond length is far longer than previously for all transition states and more for DMSO than for THF. In the same time, for the attack at the substituted carbon (**TS2**), the C_2C_3 bond is less elongated than it was without solvent. Similarly, for the attack on the nonsubstituted carbon (**TS3**), the C_1C_2 bond is also less elongated. All these results show that the transition states are "earlier" with solvent than in the gas phase.

The energetics of the reactions are given in Table 3. The reactions are less endothermic than in the gas phase, some of them become even slightly exothermic. The reaction barriers are higher. What is more interesting is to compare the barrier differences ΔE^* with and

Table 4. Barrier-Free Energies $G^*(G_{TS2}$ or $G_{TS3} - G_1)$ and $\Delta G^*(G_{TS2} - G_{TS3})$ in THF and DMSO at 298 K (in kcal/mol) with BSSE Corrections, Kinetic Constants k (in s^{-1} $(mol/L)^{-1}$), and Ratio between TS2 and TS3

		G^*_2	k_2	G^*_3	k_3	$\Delta G^*(3-2)$	ratio 3/2
a	THF	17.9	0.6	16.6	4.6	- 1.2	89/11
	DMSO	15.3	43.8	14.6	140	- 0.7	76/24
b	THF	14.4	190	19.1	0.08	4.6	0/100
	DMSO	16.6	5.4	20.2	0.01	3.6	0/100
c	THF	16.4	6.4	17.4	1.3	1.0	17/83
	DMSO	15.8	18.3	17.5	1.1	1.7	6/94

without solvent. For the methoxy−allyl (**1b**) the difference is still high and corresponds to a 100% regioselectivity in favor of the substituted carbone. For the dimethyl−allyl (**1c**) the regioselectivity is still in favor of the substituted carbon but to a lesser extent (around 80% in THF and 70% in DMSO). Finally for the methyl−allyl (**1a**) the regioselectivity is inverted and is now in favor of the nonsubstituted carbon (93% in THF and 59% in DMSO). Therefore the results obtained with solvents are in better agreement with the experimental data. Our results suggest that DMSO, compared to THF, favors the attack at the substituted carbon for **1a** and at the nonsubstituted carbon for **1c**. This trend seems verified for most ligands on Pd in the case of cyclic monomethylated allylic complexes.[33] Of course, the introduction of solvent effects by the method of continuum has limitations compared with the consideration of real solvent molecules. However it gives good qualitative results.[34]

Until now, the energy values that we discussed were calculated at 0 K like in most theoretical studies. The frequency calculations done in this work allow us to get the free energies and hence to calculate the kinetic constants for a given temperature. The results obtained at 298 K (room temperature) are given in Table 4. This temperature is often used experimentally. The kinetic constants are small, which means that the reaction is relatively slow. This has been observed experimentally: the reaction can require 16−18 h at room temperature in THF or need refluxing solvent.[2,33] The regioselectivity trend does not change much relative to the previous results, except that DMSO, compared to THF, favors the attack at the substituted carbon both for **1a** and **1c**.

4. Qualitative Interpretation

The substitution of the allyl by an electron-donating group induces a polarization of the allyl orbitals. The n and the π orbitals are polarized toward the nonsubstituted carbon (C_1) and the π^*orbital toward the substituted carbon (C_3), as shown in Scheme 3.

The greater the donating effect, the more important the polarization. The main interaction between the allyl fragment and the metal fragment $Pd(PH_3)_2$ involves the n-allyl orbital and the d_{xy} metal orbital (with the axis shown in Scheme 3). This interaction gives the HOMO and the LUMO of the whole complex. The n-orbital being polarized toward the nonsubstituted carbon C_1,

(33) Trost, B. M.; Weber, L.; Strege, P. E.; Fullerton, T. J.; Dietsche, T. J. *J. Am. Chem. Soc.* **1978**, *100*, 3416.
(34) Visentin, T. Thesis, Strasbourg, 1999. Visentin, T.; Kochanski, E.; Dedieu, A.; Moszynski, R. To be published.

Scheme 3. Shape of the Three Orbitals n, π, and π^* of an Allyl Substituted by an Electon-Donating Group

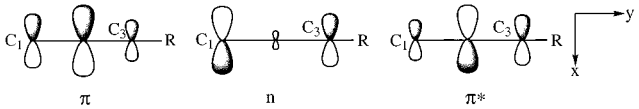

Table 5. Coefficients on C_1 and C_3 in the LUMO and HOMO of the Allyl Complexes 1a−c, in the Direction of Nucleophilic Attack, and Difference between These Coefficients (Δ)

	LUMO			HOMO		
	C_1	C_3	Δ	C_1	C_3	Δ
1a	0.70	0.74	0.04	0.29	0.47	0.18
1b	0.63	0.79	0.16	0.22	0.32	0.10
1c	0.65	0.82	0.17	0.24	0.46	0.22

the interaction is stronger between this carbon and the metal, which is reflected by a shorter PdC_1 bond length. The donor effect decreases in the order $OCH_3 > 2\ CH_3 > 1\ CH_3$, and compared to the nonsubstituted allyl complex **1d**, the PdC_1 length decreases in the order **1b** (OCH_3) < **1c** (2 CH_3) < **1a** (1 CH_3) < **1d** (Figure 1). On the contrary, the PdC_3 bond is elongated in the reverse order and the longest PdC_3 bond is obtained for **1b** (OCH_3). The lengthening of PdC_3 allows the destabilizing four-electron interaction between the π-orbital and the metal to be diminished.

When the allyl is nonsubstituted, the n-orbital and the π- and π^*-orbitals do not have the same symmetry and hence do not mix. On the contrary, when the allyl is disymmetrically substituted, the three orbitals can mix. The in-phase mixing with the π^*-orbital that is polarized toward the substituted carbon yields a larger contribution of this carbon in the LUMO orbital of the complex. The π-orbital that is polarized toward the nonsubstituted carbon yields also a larger contribution of the substituted carbon in the HOMO of the complex because the mixing is out-of-phase. The nucleophile attack takes place in the x direction roughly perpendicular to the allyl plane. We noticed in the Introduction that previous studies have suggested the frontier control of this reaction. Therefore the nucleophile HOMO interacts with both the LUMO and the HOMO of the complex, which have coefficients on the carbons in the x direction.

A large coefficient on a carbon in the LUMO favors attack at this carbon. On the contrary, a large coefficient in the HOMO increases the four-electron interactions and hence prevents the attack. Since the substituted carbon has the largest coefficient in both the LUMO and the HOMO, the site of attack results from a balance between the two effects. We must nevertheless keep in mind that the role of the LUMO is more important than that of the HOMO, which is of second order. If the difference Δ between these coefficients is considered (Table 5), one notices than for **1a** Δ is small in the LUMO; hence the substituted carbon is only a little favored. On the contrary, Δ is large in the HOMO, which favors the attack at the nonsubstituted carbon. For **1b**, Δ in the LUMO is larger than in the HOMO, which unambiguously favors the attack at the substituted carbon. For **1c**, Δ in the LUMO has the same value as for **1b**, but Δ in the HOMO is larger, which means that

the attack on the substituted carbon is still favored but less than for **1b**.

Therefore the consideration of the coefficients on the terminal carbons in the LUMO and in the HOMO allows us to give a qualitative explanation for the regioselectivity of the nucleophilic attack on a (η_3-allyl) palladium complex.

5. Conclusion

In this work, the geometries of substituted (η_3-allyl) palladium complexes were optimized with one methyl, one methoxy, and two geminal methyl groups as substituents. These complexes are disymmetrical, with the longest PdC bond on the side of the substituted carbon. The PdC bond length increases in the order CH_3 < 2 CH_3 < OCH_3. The nucleophile attack of NH_3 at these disymmetrical complexes was studied. The geometries of the resulting olefin complexes were also optimized. The transition states for the attack on both terminal carbons of the allyl moiety were localized. They are late, and their geometries look more like those of products than those of reactants. In all three cases, the energy barrier is higher for the attack at the nonsubstituted carbon, which means that attack at the substituted carbon is always favored in the gas phase.

The introduction of solvent effects by the polarizable continuum model improves largely the results compared to the experimental data. First, it allows the localization of a TS in all cases, whereas no TS were found without solvent for attack at the carbon substituted with OCH_3. With solvent, the TS are a little earlier and the energy barrier better reproduces the experimental trends. With one methyl as substituent, attack at the nonsubstituted carbon is preferred, which is experimentally found. With two geminal methyls, the nucleophilic attack is directed rather toward the substituted carbon; however the reaction is not totally regioselective (80% in THF, 70% in DMSO). Finally with a methoxy substituent, the reaction remains totally regioselective. These trends are in agreement with the experimental results mentioned in the Introduction.

An interpretation of the regioselectivity was given, based on the shape of the LUMO and HOMO of the (η_3-allyl) complex, which interact with the nucleophile HOMO. The larger the coefficient in the LUMO on a carbon in the direction of the attack, the more regioselective the reaction toward this carbon, and conversely, the larger the coefficient in the HOMO, the less regioselective the reaction. The difference between the coefficients on the two terminal carbons depends on the disymmetry of the allyl moiety, which itself depends on the electron-donating character of the substituent. The more electron donating the substituent, the more regioselective the reaction toward the substituted carbon. A similar conclusion has been reached in a recent study.[16] However, our conclusions do not take into account the steric effects. Effectively the studied substituents and the nucleophile (NH_3) are not bulky. Steric effects can reverse the regioselectivity, as it has been shown experimentally.[4,33]

We can add that the previous EHT calculations based on the comparison of the overlap populations between the nucleophile and the allylic carbons, and therefore on the coefficients in the frontier orbitals, gave very good qualitative results provided that the geometry of the allylic complex is well reproduced.

Acknowledgment. The authors thank the Pôle Scientifique de Modélisation Numérique (PSMN) at ENS-Lyon for CPU time.

OM0003032